Study of 5-*Endo* Cyclization of 5-Oxapenta-2,4-dienoyl Radical and Related Radicals by *ab Initio* Calculations. Unusual Nonradical Cyclization Mechanism

Yoshihiko Yamamoto,[†] Masatomi Ohno, and Shoji Eguchi*

Institute of Applied Organic Chemistry, Faculty of Engineering, Nagoya University, Chikusa, Nagoya 464-01, Japan

Received July 29, 1996[⊗]

5-*Endo* cyclization was shown to be remarkably effective in a 5-oxapenta-2,4-dienoyl radical by theoretical calculations as well as our previous experiments, even though a 5-*endo* closure is disfavored according to Baldwin's rule. An *ab initio* calculation suggested that this acyl radical has a flat U-shaped geometry and can be represented as a ketene-substituted α-carbonyl radical. Furthermore, the carbonyl oxygen interacts with the electron-deficient ketene group in the formation of a new σ-bond in which the radical contributes to the stabilization of the transition state as if it were a delocalized cyclopentadienyl-like radical. This nonradical cyclization mechanism was supported by IRC and spin density analyses. On the other hand, the calculated cyclizations of related radicals (*i.e.*, penta-2,4-dienoyl, 5-oxapent-4-enoyl, pent-4-enoyl, 5-oxapenta-2,4-dienyl, and penta-2,4-dienyl radicals) were shown to occur from an expected normal intramolecular addition to an olefinic or carbonyl terminus. In these cases, 5-*endo* cyclization was favored at the olefinic terminus as opposed to the carbonyl terminus. This can be explained by the different polarization of these radical acceptors toward nucleophilic radicals.

Introduction

Intramolecular ring closure of radical species is one of the most powerful tools for the synthesis of a variety of cyclic compounds.[1] In particular, the 5-*exo* cyclization of 5-hexenyl radical is well established and has been used to construct complex five-membered rings. In contrast, 5-*endo* cyclization, which is expected to be thermodynamically favorable and to also produce five-membered ring systems, has been less studied because it has been considered to be disfavored according to Baldwin's rule.[2,3] Nevertheless, some sporadic exceptions have been reported: *e.g.* 4-phenyl-4-pentenyl radical and its 5-oxa analog **1** give 5-*endo* cyclized products (Scheme 1),[4] and 2-formylbenzoyl radical **2** has been reported to participate in the photochemical rearrangement of *o*-phthalaldehyde to phthalide (Scheme 2).[5] The presence of similar 5-*endo* cyclizations has been suggested in related systems.[6] Recently, the kinetic behavior of **2** was investigated in detail by Mendenhall and co-workers, who demonstrated

Scheme 1

Scheme 2
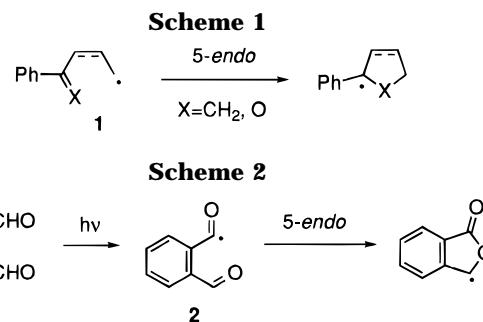
that the 5-*endo* cyclization of **2** was a highly favored process, and the rate constant ($k = 2 \times 10^8$ s^{-1} at 45 °C) was about 400 times greater than that for the 5-*exo* cyclization of the 5-hexenyl radical.[7]

Some useful synthetic methods involving 5-*endo* cyclization have been developed. Suginome and co-workers reported the oxy-radical triggered ring-opening of cyclobutanols to give ring-expanded products as the result of 5-*endo* reclosure of 5-oxapent-4-enyl radical[8] and 2-acylbenzyl radical.[9] We recently found that the treatment of 4-hydroxy-2-cyclobutenones (squaric acid derivatives) with lead tetraacetate gave 2(5*H*)-furanones (Scheme 3).[10] In this reaction, ring-opening of 4-oxo-2-cyclobutenyloxy radical (**3**, X = O) produced 5-oxapenta-2,4-dienoyl radical **4**, which underwent efficient 5-*endo* cyclization. Notably, the similar reaction of these compounds which

† Research Fellow of the Japan Society for the Promotion of Science.
⊗ Abstract published in *Advance ACS Abstracts,* December 1, 1996.
(1) (a) Beckwith, A. L. J.; Ingold, K. U. In *Rearrangements in Ground and Excited States*; de Mayo, P., Ed.; Academic Press: New York, 1980; Vol. 1, Chapter 4. (b) Surzur, J.-M. In *Reactive Intermediates*, Abramovitch, R. A. Ed.; Plenum Press: New York, 1982; Vol. 2, Chapter 3. (c) Curran, D. P. In *Comprehensive Organic Synthesis*; Trost, B. M., Ed.; Pergamon Press: Oxford, U. K., 1991; Vol. 4, Chapters 4.2.2 and 4.2.3. (d) Curran, D. P. *Synthesis* **1988**, *417*, 489. (e) Jasperse, C. P.; Curran, D. P.; Fevig, T. L. *Chem. Rev.* **1991**, *91*, 1237. (f) Curran, D. P. *Synlett* **1991**, *63*. (g) Dowd, P.; Zhang, W. *Chem. Rev.* **1993**, *93*, 2091.
(2) Baldwin's rule: Baldwin, J. E. *J. Chem. Soc., Chem. Commun.* **1976**, 734.
(3) (a) Beckwith, A. L. J.; Easton, C. J.; Serelis, A. K. *J. Chem. Soc., Chem. Commun.* **1980**, 482. (b) Beckwith, A. L. J. *Tetrahedron* **1981**, *37*, 3100. Also see refs 1a–c.
(4) (a) Bradney, M. A. M.; Forbes, A. D.; Wood, J. *J. Chem. Soc., Perkin Trans. 2* **1973**, 1655. (b) Pines, H.; Sih, N. C.; Rosenfield, D. B. *J. Org. Chem.* **1966**, *31*, 2255. (c) Wilt, J. W.; Maravetz, L. L.; Zawadzki, J. F. *J. Org. Chem.* **1966**, *31*, 3018. (d) Julia, M.; Le Goffic, F. *Bull. Soc. Chim. Fr.* **1965**, 1550 and 1555. (e) Menapace, L. W.; Kuivila, H. G. *J. Am. Chem. Soc.* **1964**, *86*, 3047.
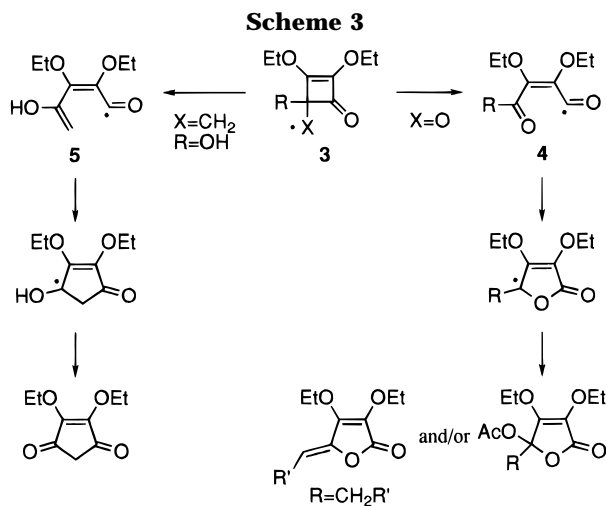(5) Harrison, D. A.; Schwartz, R. N.; Kagan, J. *J. Am. Chem. Soc.* **1970**, *92*, 5793.

(6) (a) Kende, A. S.; Belletire, J. L. *Tetrahedron Lett.* **1972**, 2145. (b) Praefcke, K. *Tetrahedron Lett.* **1973**, 973. (c) Rynard, C. M.; Thankachan, C.; Tidwell, T. T. *J. Am. Chem. Soc.* **1979**, *101*, 1196. (d) Citterio, A.; Arnoldi, A.; Minisci, F. *J. Org. Chem.* **1979**, *44*, 2674. (e) Janzen, E. G.; Oehler, U. M. *Tetrahedron Lett.* **1983**, *24*, 669.
(7) Mendenhall, G. D.; Protasiewicz, J. D.; Brown, C. E.; Ingold, K. U.; Lusztyk, J. *J. Am. Chem. Soc.* **1994**, *116*, 1718.
(8) (a) Suginome, H.; Liu, C. F.; Furusaki, A. *Chem. Lett.* **1984**, 911. (b) Suginome, H.; Liu, C. F.; Furusaki, A. *Chem. Lett.* **1985**, 27. (c) Suginome, H.; Kobayashi, K.; Itoh, M.; Furusaki, A. *Chem. Lett.* **1985**, 727. (d) Kobayashi, K.; Suzuki, M.; Sugiome, H. *J. Org. Chem.* **1992**, *57*, 599.
(9) Kobayashi, K.; Itoh, M.; Suginome, H. *Tetrahedron Lett.* **1987**, *28*, 3369.

Scheme 3

Figure 1. Energy diagram for the 5-*endo* cyclization of **6** (UHF/6-31G*).

have a radical acceptor (*e.g.* R = C≡CPh, CH=CH$_2$, and Ph) at the 4 position again gave 2(5*H*)-furanones rather than 5-*exo* cyclized products. Hence, these results imply that the 5-*endo* mode is favored over the 5-*exo* mode in these systems. Although an alternative cationic mechanism may give the same products, the thermolytic reaction of hypoiodite involving an apparent free radical pathway also exclusively gave a 5-*endo* cyclized product. Considering these results, we investigated the related cyclization of 2,4-pentadienoyl radical **5** generated from a mixed anhydride of thiohydroxamic acid and (4-oxo-2-cyclobutenyl)acetic acid (Scheme 3).[10b] Although at first it seemed more difficult for **5** to cyclize in this mode than **4**, 5-*endo* cyclization of **5** occurred prior to the competitive enol-to-keto tautomerization, to give a 4-cyclopentene-1,3-dione. Supportive semiempirical calculations (UHF/PM3) using model systems suggested that the intermediates **5** and **4** were the conjugated pentadienoyl radical and its oxa analog with a flat U-shaped geometry, which can readily cyclize to give product radicals. To obtain further insight into such 5-*endo* radical cyclizations, we performed *ab initio* calculations for various model systems.[11] In this paper we discuss in detail the 5-*endo* cyclization of penta-2,4-dienoyl and penta-2,4-dienyl radicals and their oxa and nonconjugated analogs.

Results

5-*Endo* Cyclization of 5-Oxapenta-2,4-dienoyl Radical. Prior to the *ab initio* study, the 5-*endo* cyclization of the prototypical 5-oxapenta-2,4-dienoyl radical **6** was studied using a semiempirical calculation. Using our previously reported procedure,[10b] structures of *syn*-**6**,
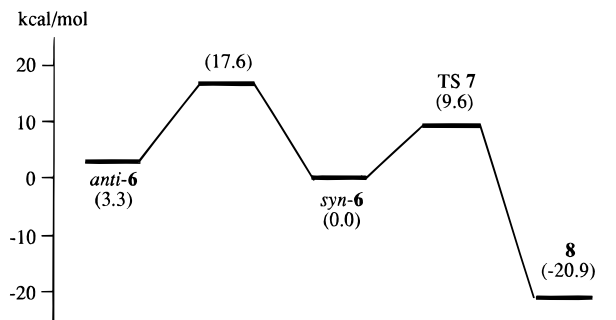
transition state (TS) **7**, and cyclized radical **8** were fully optimized at the unrestricted Hartree−Fock (UHF) level with a PM3 Hamiltonian.[12] As a result, the same planar structures as those previously reported were obtained for these radicals. Cyclization was estimated to occur with an exothermicity of $\Delta E = -11.2$ kcal/mol and an activation energy (E_a) of 9.7 kcal/mol. After establishing the predominancy of the 5-*endo* cyclization of **6** at the UHF/PM3 level, we next carried out *ab initio* calculations. When full optimizations were initially performed at the UHF/STO-3G level,[13] $E_a = 14.0$ kcal/mol ($\Delta E = -49.9$ kcal/mol) was much higher than that calculated above. To obtain more reasonable energy profiles, further calculations were carried out with the 3-21G and 6-31G* basis sets.[14,15] Whereas the energy profile obtained at the UHF/3-21G level resembled that at the UHF/PM3 level, the most reliable result was obtained with the 6-31G* basis set: In this case, $\Delta E = -20.9$ kcal/mol and $E_a = 9.6$ kcal/mol. In addition, *syn*-**6**, a preferable conformer for 5-*endo* cyclization, was found to be 3.3 kcal/mol more stable than *anti*-**6** (Figure 1). The calculated energies and structural data are summarized in Tables 1 and 2, respectively.

Figure 2 shows the optimized structures of *syn*-**6**, TS **7**, and **8** at the UHF/6-31G* level. *syn*-**6** has a flat U-shaped geometry, in which the C(1) atom is almost *sp*-hybridized (∠C(2)−C(1)−O(6) = 174.5°). Therefore, **6** is a delocalized π-radical rather than a localized acyl radical. TS **7** also has a completely planar structure, in which the length of the newly formed C(1)−O(5) bond is shortened to 1.920 Å and the C(2)−C(1)−O(6) angle is decreased to 154.5°. The cyclized radical **8** is planar and lowest in energy. These results are reminiscent of a Nazarov-type cyclization rather than the intramolecular addition of an acyl radical to a carbonyl moiety. Additional details on the transition structure are described in the next section. Houk *et al.* discussed the analogous pattern of cationic and anionic pentadienyl → cyclopentenyl rearrangements using *ab initio* calculations.[16]

Previously, Mendenhall and co-workers suggested that conformations of the acyl radical intermediate play an

(10) (a) Yamamoto, Y.; Ohno, M.; Eguchi, S. *J. Org. Chem.* **1994**, *59*, 4707. (b) Yamamoto, Y.; Ohno, M.; Eguchi, S. *J. Am. Chem. Soc.* **1995**, *117*, 9653.

(11) For examples of theoretical calculations on radical reactions; (a) Hoyland, J. R. *Theor. Chim. Acta* **1971**, *22*, 229. (b) Bonacic-Koutecky, V.; Salem, L. *J. Am. Chem. Soc.* **1977**, *99*, 842. (c) Riemenschneider, K.; Bartels, H.; Eichel, W.; Boldt, P. *Tetrahedron Lett.* **1979**, 189. (d) Bischof, P. *Helv. Chim. Acta* **1980**, *63*, 1434. (e) Lee, I.; Lee, B. S.; Song, C. H.; Kim, C. K. *Bull. Kor. Chem. Soc.* **1982**, *4*, 84. (f) Caramella, P.; Rondan, N. G.; Paddon-Row, M. N.; Houk, K. N. *J. Am. Chem. Soc.* **1981**, *103*, 2438. (g) Paddon-Row, M. N.; Rondan, N. G.; Houk, K. N. *J. Am. Chem. Soc.* **1982**, *104*, 7162. (h) Houk, K. N.; Paddon-Row, M. N.; Spellmeyer, D. C.; Rondan, N. G.; Nagase, S. *J. Org. Chem.* **1986**, *51*, 2874, and references cited therein. (i) Spellmeyer, D. C.; Houk, K. N. *J. Org. Chem.* **1987**, *52*, 959. (j) Zipse, H.; He, J.; Houk, K. N.; Giese, B. *J. Am. Chem. Soc.* **1991**, *113*, 4324. (k) Damm, W.; Giese, B.; Hartung, J.; Hasskerl, T.; Houk, K. N.; Hüter, O.; Zipse, H. *J. Am. Chem. Soc.* **1992**, *114*, 4067. (l) Takeuchi, Y.; Kawahara, S.; Suzuki, T.; Koizumi, T.; Shinoda, H. *J. Org. Chem.* **1996**, *61*, 301.

(12) Stewart, J. P. *Comput. Chem.* **1989**, *10*, 221.

(13) STO-3G: Hehre, W. J.; Stewart, R. F.; Pople, J. A. *J. Chem. Phys.* **1969**, *51*, 2657.

(14) 3-21G: (a) Binkley, J. S.; Pople, J. A.; Hehre, W. J. *J. Am. Chem. Soc.* **1980**, *102*, 939. (b) Gordon, M. S.; Binkley, J. S.; Pople, J. A.; Pietro, W. J.; Hehre, W. J. *J. Am. Chem. Soc.* **1982**, *104*, 2797. (c) Pietro, W. J.; Frand, M. M.; Hehre, W. J.; DeFrees, D. J.; Pople, J. A.; Binkley, J. S. *J. Am. Chem. Soc.* **1982**, *104*, 5039.

(15) 6-31G*: (a) Hariharan, P. C.; Pople, J. A. *Chem. Phys. Lett.* **1972**, *66*, 217. (b) Frand, M. M.; Pietro, W. J.; Hehre, W. J.; Binkeley, J. S.; DeFrees, D. J.; Pople, J. A. *J. Chem. Phys.* **1982**, *77*, 3654.

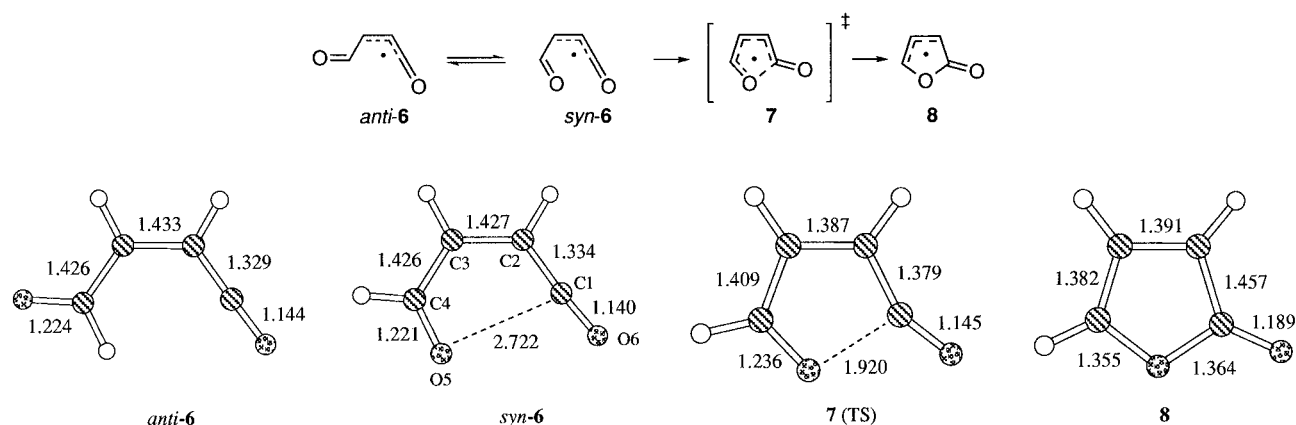(16) Houk, K. N.; Li, Y.; Evanseck, J. D. *Angew. Chem., Int. Ed. Engl.* **1992**, *31*, 682.

Figure 2. Optimized geometries of radicals *anti*-**6**, *syn*-**6**, and **8**, and transition state **7** (UHF/6-31G*). Indicated values show the bond length in angstroms (Å).

Table 1. Calculated Energies of Radicals 6 and 8, and Transition State 7, and Imaginary Frequencies

| methods	*syn*-**6**	*anti*-**6**	TS **7**	imaginary frequency	**8**
UHF/PM3	−29.3 kcal/mol (0.0)[a]		−19.6 kcal/mol (9.7)[a]	$630i\,\text{cm}^{-1}$	−40.6 kcal/mol (−11.3)[a]
UHF/STO-3G	−298.9559 au (0.0)[a]		−298.9336 au (14.0)[a]	$473i\,\text{cm}^{-1}$	−299.0354 au (−49.9)[a]
UHF/3-21G	−301.1922 au (0.0)[a]		−301.1745 au (11.1)[a]	$888i\,\text{cm}^{-1}$	−301.2225 au (−19.0)[a]
UHF/6-31G*	−302.8860 au (0.0)[a]	−302.8579 au (3.3)[a]	−302.8707 au (9.6)[a]	$668i\,\text{cm}^{-1}$	−302.9193 au (−20.9)[a]

[a] Relative energies (kcal/mol) are given in parentheses.

Table 2. Bond Length (Å) and the C(2)−C(1)−O(6) Angle for the Transition Structure of 5-*endo* Cyclization of 6

method	C(1)−C(2)	C(2)−C(3)	C(3)−C(4)	C(4)−O(5)	O(5)−C(1)	C(1)−O(6)	∠C(2)−C(1)−C(6)
UHF/PM3	1.392	1.391	1.432	1.258	1.933	1.171	159.0
UHF/STO-3G	1.381	1.406	1.411	1.315	1.801	1.206	153.4
UHF/3-21G	1.372	1.386	1.405	1.264	1.916	1.165	155.6
UHF/6-31G*	1.379	1.387	1.409	1.236	1.920	1.145	154.5
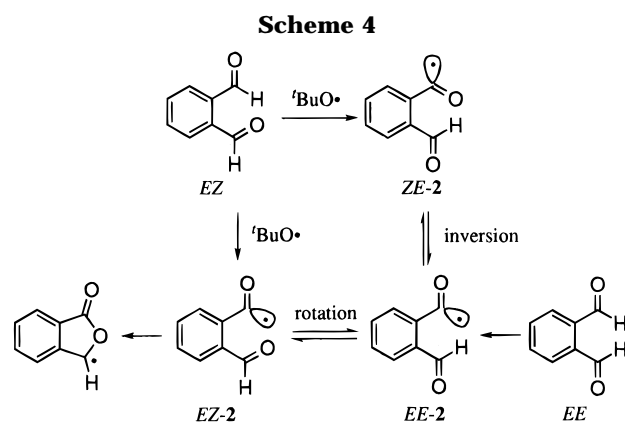
Scheme 4

Scheme 5

important role in the 5-*endo* closure of analogous benzo-fused radical **2** (Scheme 4).[7] A preferable conformer (*EZ*)-**2** can be produced either by direct H-abstraction from (*EZ*)-phtalaldehyde or indirectly by inversion/rotation of conformers (*ZE*)-**2** and (*EE*)-**2** from either (*EZ*)- or (*EE*)-phthalaldehyde. In this respect, related *syn*-**6** is considered a delocalized radical based on our calculations, and the possibility of such inversion may be ruled out. Furthermore, *syn*-**6** was calculated to be 3.3 kcal/mol more stable than *anti*-**6** with a C(3)−C(4) bond-rotation barrier of 17.6 kcal/mol. For comparison, the 5-*endo* cyclization of benzo analog **2** was also examined by *ab initio* calculations at the UHF/6-31G* level (Scheme 5). As expected, the 2-formylbenzoyl radical **2** was also shown to have a delocalized and flat U-shaped structure, with the C(1) atom almost *sp*-hybridized (∠C(2)−C(1)−O(6) = 173.2°). The 5-*endo* cyclization of **2** was estimated to occur with $\Delta E = -27.3$ kcal/mol and $E_a = 12.4$ kcal/mol. The benzo-fused radical also shows delocalization
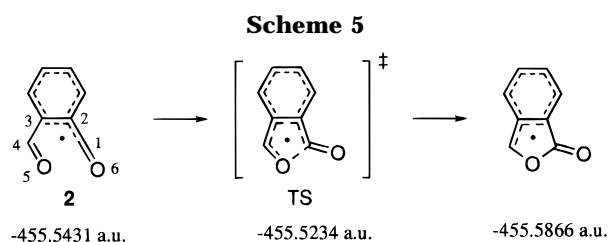
of the 3-phthalidyl radical into a phenyl ring. Thus, **2** has an energy profile of radical cyclization similar to that of **6**.

5-*Endo* Cyclization of Penta-2,4-dienoyl Radical. In conjunction with the above successful 5-*endo* cyclization of 5-oxapenta-2,4-dienoyl radical, we previously reported a similar cyclization of 4-hydroxypenta-2,4-dienoyl radical (Scheme 3).[10b] We now examine more precisely the cyclization of a model penta-2,4-dienoyl radical **9** at the UHF/6-31G* level. Figure 3 shows optimized geometries of starting radical **9**, transition state **10**, and cyclized radical **11**. Whereas radical **9** has a flat U-shaped geometry similar to that of *syn*-**6**, the most notable difference is that the distance of C(1)−C(5) (3.170 Å) is considerably longer than that of C(1)−C(5) in *syn*-**6**. This is because H(11) is in close proximity to C(1), and threfore the C(5) terminus is moved away from the acyl radical center to reduce steric interaction. In proceeding from **9** to transition state **10**, the initial planar structure is slightly distorted (∠C(1)−C(2)−C(3)−C(4) = 18.5° and ∠C(2)−C(3)−C(4)−C(5) = 6.1°), while the C(5) atom is rotated (∠C(5)−C(1)−H(11) = 78.6°) and the C(2)−C(1)−O(6) angle is decreased to 130.7°. The estimated $E_a = 21.7$ kcal/mol indicates that cyclization of the penta-2,4-dienoyl radical **9** is kinetically less favorable
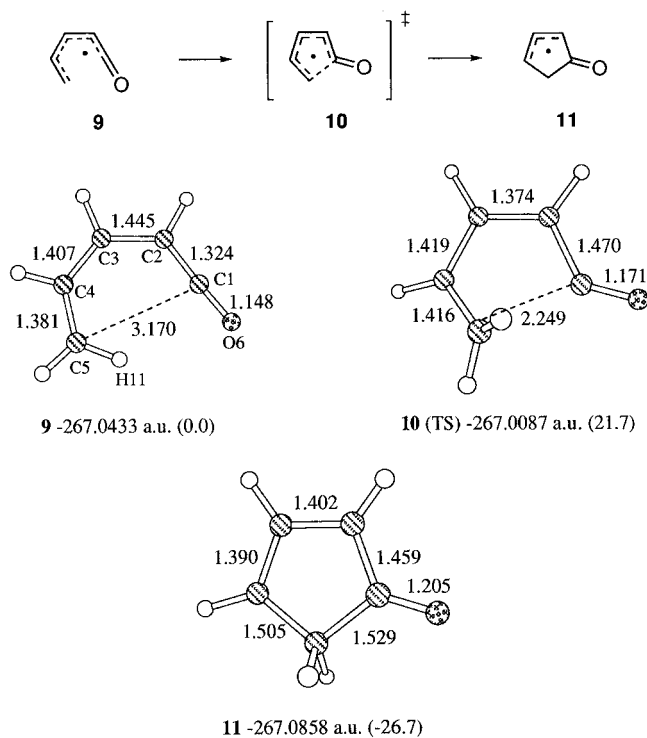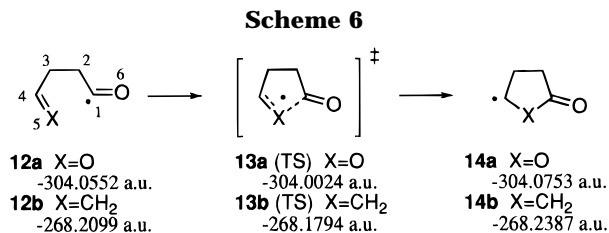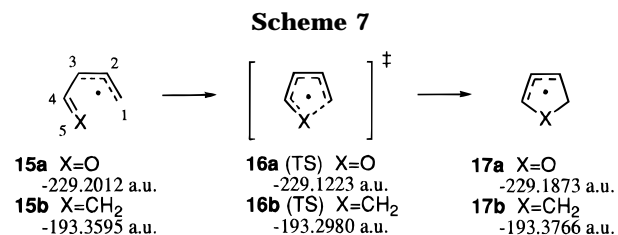
9 -267.0433 a.u. (0.0)   10 (TS) -267.0087 a.u. (21.7)

11 -267.0858 a.u. (-26.7)

Figure 3. Optimized geometries and energies of radicals **9** and **11**, and transition state **10** (UHF/6-31G*). Indicated values show the bond length in angstroms (Å), and relative energies are given in parentheses (kcal/mol).

Scheme 6

12a X=O
-304.0552 a.u.
12b X=CH$_2$
-268.2099 a.u.

13a (TS) X=O
-304.0024 a.u.
13b (TS) X=CH$_2$
-268.1794 a.u.

14a X=O
-304.0753 a.u.
14b X=CH$_2$
-268.2387 a.u.

than that of the oxa-analog of **6**. This may be due to different interaction of the reacting centers during cyclization. Despite the common U geometry of the starting radicals **6** and **9**, the acyl radical character is enhanced in the transition structure of **10** (the C(2)−C(1)−O(6) angle is close to the standard carbonyl angle), which resembles that from the nonconjugated analog (*i.e.*, **13**: *vide infra*) rather than that from the oxa-analog (*i.e.*, **7**: *vide supra*).

Influence of Conjugation on Acyl Radical Cyclization. The above cases all involve a double bond between the acyl radical center and the reacting terminus, which produces *cis*-geometry and full conjugation in the molecule. If this condition is applied to a nonrestricted saturated system, substantial differences may be observed. Therefore, the related cyclization of 5-oxapent-4-enoyl radical **12a**[17] was investigated. The heats of formation of starting radical **12a**, transition state **13a**, and cyclized radical **14a** are shown in Scheme 6. The lack of conjugation might impose a great disadvantage on this cyclization, since the C(2)−C(3) bond rotates freely and the product radical **14a** is less stable. In fact, the acyl radical center is located far away from the
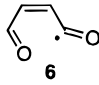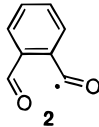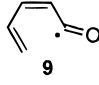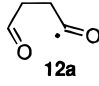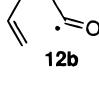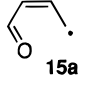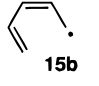
---

(17) In relation to the rearrangement of 4-oxo-2-cyclobutenyloxy radical (Scheme 4), we also attempted the ring-opening reaction of 2-oxocyclobutyloxy radical, in which 5-*endo* cyclization of 5-oxapent-4-enyl radical intermediates gave 4-acetoxybutanolides (ref 10).

Scheme 7

15a X=O
-229.2012 a.u.
15b X=CH$_2$
-193.3595 a.u.

16a (TS) X=O
-229.1223 a.u.
16b (TS) X=CH$_2$
-193.2980 a.u.

17a X=O
-229.1873 a.u.
17b X=CH$_2$
-193.3766 a.u.

carbonyl group in the conformer of **12a** with the lowest energy. A cyclizable local minimum of **12a** undergoes 5-*endo* cyclization *via* transition state **13a** with higher activation energy (33.1 kcal/mol) and lower exothermicity (12.6 kcal/mol). Obviously, cyclization is less favored in a saturated system than in unsaturated systems such as **2** and **6**. In contrast, the analogous pent-4-enoyl radical **12b** was more readily cyclized than the comparative 5-oxa radical **12a**. Scheme 6 shows the calculated heats of formation for the corresponding states **12b**, **13b**, and **14b** at the UHF 6-31G* level. Despite free rotation of the C(2)−C(3) bond, 5-*endo* cyclization of **12b** was estimated to proceed with E_a = 19.1 kcal/mol, which was even less than that required for the unsaturated system **9**. The contrast in the reactivities of these saturated analogs (**12a** *vs* **12b**) is seemingly unexpected, but reasonable since they cyclize through the usual intramolecular radical addition, in which **12b** benefits due to flexibility of the molecule (see also the next section).

Influence of Radical Characteristics on Cyclization. All of the cyclizations demonstrated above involved acyl radical intermediates. We next focused on the effect of the characteristics of the radical on the efficacy of 5-*endo* cyclization. If the acyl radical center is replaced by an alkyl radical, the electronic and structural changes should be reflected in *ab initio* calculations; naturally a ketenic form is no longer involved, and the nucleophilic nature and rotational motion will be different. A model system, 5-oxapenta-2,4-dienyl radical **15a**, showed results dramatically different than those with the acyl radical. Scheme 7 shows the calculated heats of formation for starting radical **15a**, transition state **16a**, and cyclized radical **17a** at the UHF/6-31G* level. The alkyl radical **15a** is again a delocalized radical with a flat U-shaped structure, but the C(1)−O(5) distance is rather long (3.020 Å) because of steric repulsion between O(5) and H(6). Progression from **15a** to the transition state **16a** produces a slight distortion (∠C(1)−C(2)−C(3)−C(4) = 19.3° and ∠C(2)−C(3)−C(4)−O(5) = 1.0°) and rotation at C(1) (∠O(5)−C(1)−H(6) = 81.0°). The calculated activation energy of 49.5 kcal/mol is 5 times larger than that for the corresponding acyl radical **6**, and the fact that it is also 8.7 kcal/mol less endothermic is also apparently an unfavorable factor; the C(1)−O(5) distance in *syn*-**6** is shorter than that in **15a**, and enone conjugation stabilizes cyclized radical **8**, but not **17a**. Thus, these kinetic and thermodynamic differences confirmed the superiority of the acyl radical **6** in 5-*endo* cyclization. Finally, the same *ab initio* calculation was applied to the cyclization of penta-2,4-dienyl radical **15b**, an extreme variant of the initial radical **6** (Scheme 7). A theoretical study of related cationic and anionic pentadienyl ↔ cyclopentenyl rearrangements was carried out by Houk *et al.*[16] For the cationic rearrangement, conrotatory electrocyclic ring closure is calculated to be a highly exothermic process (−27 kcal/mol) with an activation energy of nearly zero (MP2/6-31G*). In the transition structure, the newly formed bond is 2.268 Å long, and

Table 3. Activation Energies (E$_a$), Partial Bond Lengths, and Relative Energies (ΔE) for 5-*Endo* Cyclization of 6, 2, 9, 12a, 12b, 15a, and 15b

| Starting radical	E$_a$ (kcal/mol)	Partial bond length in TS (Å)	ΔE^a (kcal/mol)
6	9.6	1.920	−20.9
2	12.4	1.815	−27.3
9	21.7	2.249	−26.7
12a	33.1	1.952	−12.6
12b	19.1	2.204	−18.1
15a	49.5	2.028	8.7
15b	38.6	2.286	−10.7

$^a \Delta E = \Delta H_{f,\text{cyclized radical}} - \Delta H_{f,\text{starting radical}}$

all of the partial double bonds have identical bond lengths of 1.389 Å. On the other hand, in the transition state of the disrotatory electrocyclic ring-opening from cyclopentenyl anion to pentadienyl anion, the newly formed bond is 2.181 Å long and the lengths of the terminal and internal partial double bonds are 1.394 and 1.435 Å, respectively. In contrast to these electrocyclic reactions, the unsymmetrical transition structure **16b**, in which all of the partial double bonds have different lengths, achieves ring closure through the intramolecular addition of the alkyl radical [C(1)] to the diene terminus [C(5)]; the C(1) center is rotated ($\angle$H(6)−C(1)−C(2)−C(3) = 97.3°) and the C(1)−C(2) bond length is extended from 1.374 Å to 1.490 Å, whereas the C(4)−C(5) bond still retains an olefinic character (C(4)−C(5) = 1.419 Å, $\angle$H(12)−C(5)−C(4)−C(3) = 154.3°, $\angle$H(12)−C(5)−C(4)H(10) = −12.2°). Compared with the above cationic cyclization, radical cyclization from **15b** to **17b** is less exothermic (−10.7 kcal/mol) and has a greater activation energy (38.6 kcal/mol). With regard to radical cyclization, the pentadienyl radical **15b** is inferior to the pentadienoyl radical **9** from both kinetic and thermodynamic perspectives.

Discussion

The estimated E_a and ΔE values based on 6-31G* *ab initio* calculations are summarized in Table 3. Spin contamination by states of higher multiplicity, which may
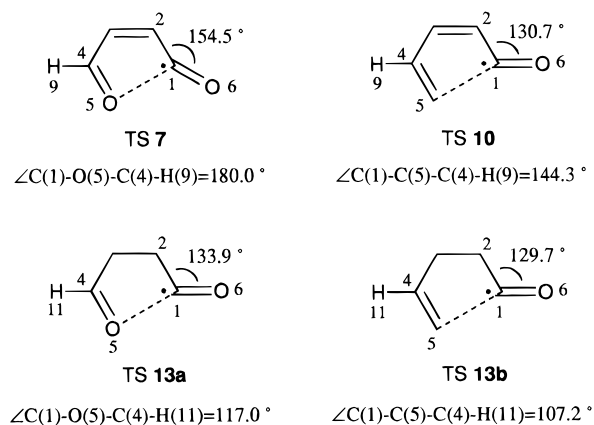
Figure 4. Transition states of 5-*endo* cyclization of acyl radicals **6**, **9**, **12a**, and **12b**.

arise since the UHF wave functions are not pure doublet states, do not appear to be significant; in fact, for the transition states studied here, S^2 ranges from 0.76 to 1.50 whereas $S^2 = 0.75$ for a pure doublet state (see supporting information). Furthermore, the ROHF/6-31G* calculations for the 5-*endo* cyclization of **6** showed similar energy profiles (E_a = 5.3 kcal/mol and $\Delta E = -15.5$ kcal/mol) and geometries for **6**, TS **7**, and **8**. These results suggest that the 5-*endo* cyclization of 5-oxapenta-2,4-dienoyl radical **6** is the most favorable process among all of the radicals surveyed in this report. The flat U-shaped geometry of *syn*-**6** is entropically ideal for cyclization (this is associated with Nazarov cyclization), and the resulting radical **8** is stable enough due to enone conjugation (its resonance form is a furyloxy radical) to give a thermodynamic advantage. On the other hand, the related cyclization, for example, of penta-2,4-dienoyl radical **9** proceeds with a preferable flat U-shape, but is energetically less favorable. In fact, this cyclization was estimated to occur with an activation energy comparable to that of the simple intramolecular addition of pent-4-enoyl radical **12b**. Furthermore, a nonconjugated analog (5-oxapent-4-enyl radical **12a**) was estimated to cyclize with much higher energy. Comparison of the transition states intuitively shows that the ring closure of **6** is unique (Figure 4). Cyclization of nonconjugated systems such as **12a** and **12b** is a normal intramolecular addition with transition structures **13a** and **13b** (the dihedral angles $\angle$C(1)−O(5)−C(4)−H(11) and $\angle$C(1)−C(5)−C(4)−H(11) are nearly 110° and $\angle$C(2)−C(1)−O(6) is nearly 130°).[18] A similar transition structure with less inclination at C(5) was obtained for the cyclization of **9**. In contrast, the transition structure **7** for the cyclization of **6** has a completely planar geometry (the dihedral angle $\angle$C(1)−C(5)−C(4)−H(9) is 180°) and the C(2)−C(1)−O(6) angle of 154.5° is larger than that found in **10**, **13a**, and **13b**. Therefore the 5-*endo* cyclization of **6** seems to be a very special case.

To obtain more detailed insight into the mechanisms involved, we next performed an intrinsic reaction coordinate (IRC)[19] analysis for the ring closure of **6**. IRC analysis was carried out at the UHF/3-21G level, and the

(18) In these transition structures, the angles of attack of the radical are about 57° for TS **13b**, and 50° for TS **13a**, which are considerably smaller than the ideal tetrahedral angle of 109° (ref 11h). An angle of attack (106°) which is close to the ideal angle was reported for the 5-*exo* cyclization of 5-hexenyl radical (ref 11i).

(19) (a) Fukui, K. *Acc. Chem. Res.* **1981**, *14*, 363. (b) Schmidt, M. W.; Gordon, M. S.; Dupuis, M. *J. Am. Chem. Soc.* **1985**, *107*, 2585.
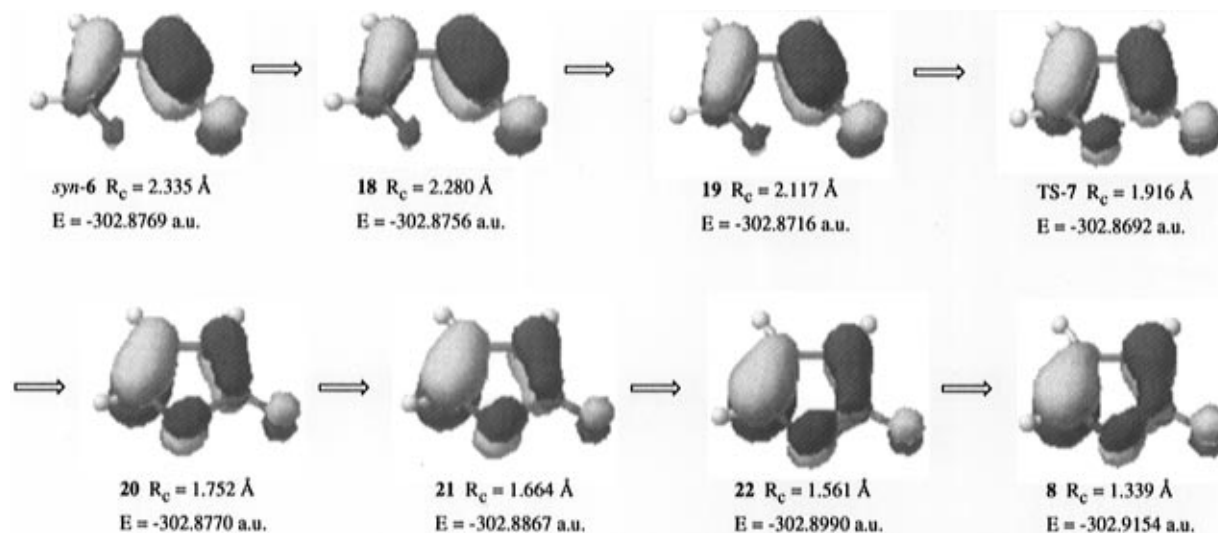
syn-**6** $R_c = 2.335$ Å
E = -302.8769 a.u.

18 $R_c = 2.280$ Å
E = -302.8756 a.u.

19 $R_c = 2.117$ Å
E = -302.8716 a.u.

TS-**7** $R_c = 1.916$ Å
E = -302.8692 a.u.

20 $R_c = 1.752$ Å
E = -302.8770 a.u.

21 $R_c = 1.664$ Å
E = -302.8867 a.u.

22 $R_c = 1.561$ Å
E = -302.8990 a.u.

8 $R_c = 1.339$ Å
E = -302.9154 a.u.

Figure 5. Calculated structures, energies, reaction coordinates (R_c), and SOMOs of representative intermediates in the IRC of the 5-*endo* cyclization of **6** (UHF/6-31G*//UHF/3-21G).

α-MO20 (-12.22 eV)   α-MO21 (-12.13 eV)   α-MO22 (-8.22 eV)   α-MO23 (3.79 eV)   α-MO24 (5.06 eV)

β-MO20 (-11.96 eV)   β-MO21 (-10.27 eV)   β-MO22 (0.94 eV)   β-MO23 (5.20 eV)   β-MO24 (5.71 eV)
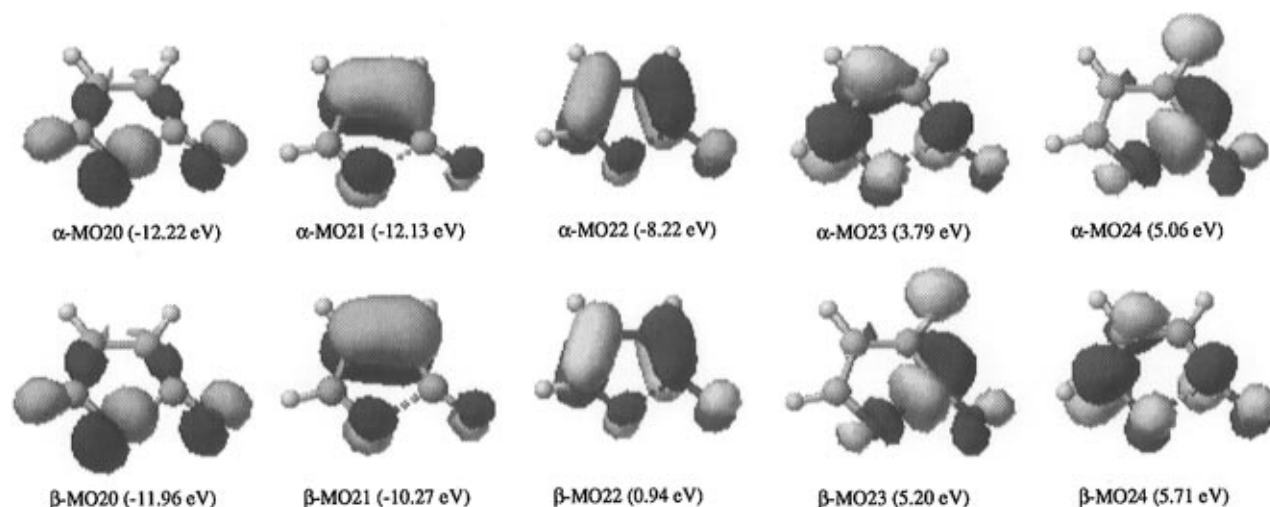
Figure 6. Molecular orbitals with eigenvalues of TS **7** (UHF/6-31G*//UHF/3-21G).

energies of representative intermediates were calculated at the UHF/6-31G*//UHF/3-21G level. The resulting structures of these intermediates are depicted with the singly occupied molecular orbitals (SOMOs) in Figure 5. As shown, the SOMOs are perpendicular to the molecular plane and their symmetry is unchanged throughout the reaction. The delocalized radical does not participate in C(1)−O(5) bond formation but does contribute to the stabilization of the system to maintain a flat U-shape geometry. In addition, the molecular orbitals of transition state **7** depicted in Figure 6 suggest an unusual nonradical mechanism; among these orbitals, the 20th molecular orbitals occupied by α- and β-spin electrons (α-MO20 and β-MO20) have similar energy levels and the same symmetry. These correspond to the nonbonding orbital of a carbonyl oxygen lone pair of electrons. Similarly, unoccupied molecular orbitals, α-MO24 and β-MO23, correspond to the antibonding orbital of ketene carbonyl. Interaction of the lone pair orbital on O(5) with the empty *p*-orbital on C(1) in close proximity allows for the formation of a new σ-bond. Consequently, as illustrated in Scheme 8, the net cyclization is best explained by nonradical ring closure from ketene-substituted α-carbonyl radical *syn*-**6**[20] to the cyclized radical **8**, with TS **23** represented as a dipolar π-radical stabilized

Scheme 8

syn-**6**   TS **23**   **8**
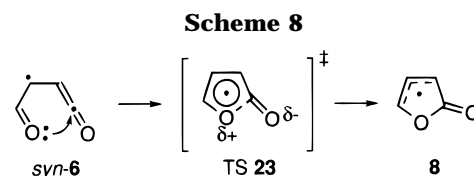
transition structure. This mechanism is also supported by spin density calculations (Table 4). In *syn*-**6**, the highest α-spin population lies one C(3). Upon progression to transition state **7**, this radical is appreciably delocalized to give comparable spin densities on carbon and oxygen atoms, which is reminiscent of a delocalized cyclopentadienyl-like radical, and is consistent with the proposed transition structure TS **23**. In the cyclized radical **8**, the stable allylic radical has a high α-spin population on C(2) and C(4).

IRC and spin density analyses for **9** were carried out in the same manner and the results are shown in Figure 7 and Table 5. In sharp contrast to the case with **6**, the SOMO changes dramatically throughout the reaction. Like *syn*-**6**, **9** is considered to be a ketene-substituted allylic radical[20] with high α-spin populations on C(3) and

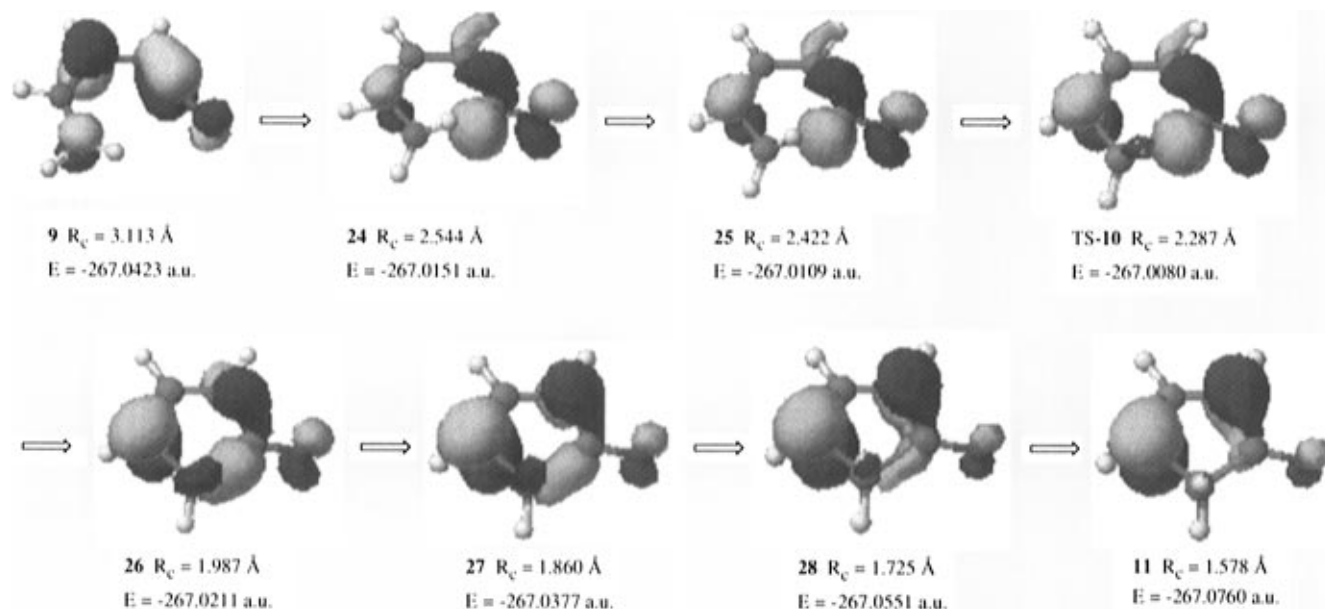(20) For an example of a ketene-substituted radical; Weinberg, J. S.; Miller, A. *J. Org. Chem.* **1979**, *44*, 4722.

9 $R_c = 3.113$ Å   **24** $R_c = 2.544$ Å   **25** $R_c = 2.422$ Å   **TS-10** $R_c = 2.287$ Å
$E = -267.0423$ a.u. $E = -267.0151$ a.u. $E = -267.0109$ a.u. $E = -267.0080$ a.u.

26 $R_c = 1.987$ Å   **27** $R_c = 1.860$ Å   **28** $R_c = 1.725$ Å   **11** $R_c = 1.578$ Å
$E = -267.0211$ a.u. $E = -267.0377$ a.u. $E = -267.0551$ a.u. $E = -267.0760$ a.u.

Figure 7. Calculated structures, energies, reaction coordinates (R_c), and SOMOs of representative intermediates in the IRC of the 5-*endo* cyclization of **9** (UHF/6-31G*//UHF/3-21G).

Table 4. Spin Densities of Representative Intermediates in the IRC of the 5-*Endo* Cyclization of 6

atom	*syn*-**6**	**18**	**19**	TS-**7**	**20**	**21**	**22**	**8**
C(1)	0.2634	0.2594	0.2336	0.0424	−0.1824	−0.2741	−0.3413	−0.3548
C(2)	−0.3151	−0.3078	−0.2550	0.1784	0.6198	0.7480	0.8269	0.8802
C(3)	0.8674	0.8548	0.7775	0.2333	−0.3302	−0.5037	−0.6104	−0.6855
C(4)	−0.5076	−0.4789	−0.3190	0.2495	0.5848	0.6948	0.7686	0.8314
O(5)	0.6116	0.5887	0.4624	0.1110	0.0282	0.0093	−0.0076	−0.0331
O(6)	0.1015	0.1066	0.1322	0.2460	0.3507	0.3998	0.4404	0.4412

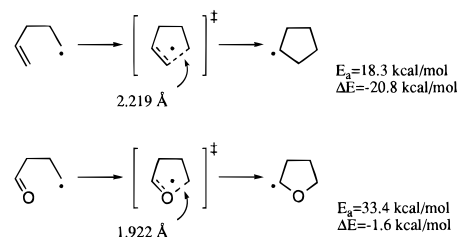**Table 5. Spin Densities of Representative Intermediates in the IRC of the 5-*Endo* Cyclization of 9**

atom	**9**	**24**	**25**	TS-**10**	**26**	**27**	**28**	**11**
C(1)	0.3599	0.6053	0.5699	0.4996	−0.1086	−0.4278	−0.5224	−0.5308
C(2)	−0.4444	0.7153	0.7463	0.7879	0.8762	0.9108	0.9266	0.9333
C(3)	0.9779	−0.6835	−0.7033	−0.7247	−0.7627	−0.7796	−0.7831	−0.7797
C(4)	−0.7915	0.7995	0.8704	0.9444	0.9951	0.9851	0.9784	0.9670
C(5)	0.9683	−0.8267	−0.8831	−0.9091	−0.3967	−0.1332	−0.0837	−0.0685
O(6)	0.0689	0.2986	0.3050	0.3088	0.3947	0.4843	0.5393	0.5400

C(5). As the reaction proceeds, C(5) is rotated and C(1) is rehybridized from *sp* to *sp²* (*i.e.*, the C(2)−C(1)−O(6) angle is decreased) to impose an acyl radical character, which allows interaction with C(5) to form a new σ-bond. At that time, the α-spin population at C(1) is first increased but then decreased after the transition state, while those at C(2) and C(4) are increased gradually. Thus, this ring closure is considered a normal intramolecular addition of an acyl radical to a diene. Cyclization of the nonconjugated acyl radicals **12a** and **12b** is a simple case of this type. IRC and spin density analyses (see supporting information) clearly show that **12a** and **12b** are localized *sp²* acyl radicals and the α-spin population is overwhelmingly high at C(1). The SOMOs change expectedly along the IRC to form the radical *p*-lobe on C(4), at which the α-spin population is gradually increased. Essentially, the cyclizations of **9** and **12b** resemble each other.

In addition to the different mode of cyclization, the different reactivity observed in normal radical cyclizations is also interesting. The more nucleophilic acyl radical **12a** attacks a *p*-orbital of the carbonyl oxygen, as judged from ∠C(1)−O(5)−C(4)−H(11) = 117°. In contrast, the less nucleophilic alkyl radical **15a** attacks an *n*-orbital of the carbonyl oxygen, as judged from the nearly planar transition state **16a** (see supporting infor-

mation). The estimated difference in reactivity between **9** and **12b** also seems to be associated with a stereochemical source at the reactive end. In the case of an olefinic terminus, rotation at the C(5) end is needed to form a new σ-bond. Such motion is favored in a flexible system such as **12b**, which explains why **12b** undergoes cyclization more readily than **9**. However, a similar trend is not seen for **6** *vs* **12a** because of the exceptional behavior of **6**. Finally, we should mention the radicophilicity of an acceptor group. As seen in Table 3, an olefinic terminus shows a better reactivity than a carbonyl group (*i.e.*, **12a** *vs* **12b** and **15a** *vs* **15b**),[21] except for the unusual case of **6** *vs* **9**. This tendency may originate from the

(21) The calculation at the UHF/6-31G* level revealed the same tendency for the prototypical cyclizations shown below. Notably, the estimated $E_a = 18.3$ kcal/mol for the cyclization of 4-pentenyl radical was consistent with the experimental value of $E_a = 18 \pm 3$ kcal/mol; Watkins, K. W.; Olsen, D. K. *J. Phys. Chem.* **1972**, *76*, 1089.

2.219 Å $E_a = 18.3$ kcal/mol $\Delta E = -20.8$ kcal/mol

1.922 Å $E_a = 33.4$ kcal/mol $\Delta E = -1.6$ kcal/mol

polarization of the acceptor. The electronegative oxygen site of the carbonyl group is considered not to be preferable toward nucleophilic acyl and alkyl radicals; however, this effect is not significant at the nonpolarized olefinic carbon.

Summary

Radical 5-*endo* cyclization was surveyed using an *ab initio* calculation (UHF/6-31G*) for various model systems including 5-oxapenta-2,4-dienoyl radical **6** and penta-2,4-dienoyl radical **9** and their analogs such as a benzo-fused radical **2**, nonconjugated radicals **12a** and **12b**, and alkyl radicals **15a** and **15b**. The results indicated that the 5-*endo* cyclization of **6** is a kinetically and thermodynamically favorable process with the following features: (1) the conformer of the starting radical with the lowest energy has a flat U-shaped geometry, which is entropically favorable for cyclization, (2) ring closure occurs due to the intramolecular addition of a carbonyl oxygen to a ketene moiety rather than from simple acyl radical addition to a carbonyl group, and (3) the cyclized radical is stabilized with conjugation, which offers thermodynamic advantages. The transition structure TS **23** was examined by IRC and spin density analyses. The radical **6** is considered to be a ketene-substituted α-carbonyl radical, and interaction between carbonyl and ketene groups is responsible for the formation of a new σ-bond, where the radical helps to stabilize the transition state as if it were a delocalized cyclopentadienyl-like radical. Cyclization of the benzo-fused radical **2** has an energy profile similar to that of **6**.

Except for **2** and **6**, the other radicals analyzed cyclized through a normal intramolecular addition to an olefinic or carbonyl terminus. These cases show the following noteworthy features: (1) an olefinic terminus shows better radicophilicity than a carbonyl terminus (*i.e.*, **12a** *vs* **12b** and **15a** *vs* **15b**) because of the intrinsic nucleophilicity of acyl and alkyl radicals, (2) a nonconjugated radical is more readily cyclized (*i.e.*, **9** *vs* **12b**) due to its motional flexibility, and (3) an *n*-orbital of the carbonyl terminus, rather than a *p*-orbital, participates in **15a**.

Computational Methods

Semiempirical calculations (UHF/PM3[13]) were carried out using MOPAC software Version 94.10 in CAChe Version 3.7. The eigenvector-following (EF) method was used for full optimization of stationary geometries and to compute the heats of formation using the keyword PRECISE. *Ab initio* calculations were carried out using Mulliken software Version 1.1.0 with the CAChe Mulliken interface. All stationary geometries were obtained by UHF or RHF SCF calculations with the specified basis set (STO-3G,[13] 3-21G,[14] and 6-31G*[15]). The resulting transition structures were subjected to a vibrational analysis, and in each case, only one imaginary frequency was found. IRC[19] calculations were first performed at the UHF/3-21G level, and the heats of formation of the resulting intermediates were further computed at the UHF/6-31G* level.